

# Expectations from Realistic Microlensing Models of M31. I: Optical Depth

Geza Gyuk<sup>1</sup> and Arlin Crotts<sup>2</sup>

<sup>1</sup>*Department of Physics, University of California, San Diego, 9500 Gilman Drive, La Jolla, CA 92093*

<sup>2</sup>*Department of Astronomy, Columbia University, 550 W. 120th St., New York, NY 10027*

Received \*\*\*

## ABSTRACT

We provide a set of microlensing optical depth maps for M31. Optical depths towards Andromeda were calculated on the basis of a four component model of the lens and source populations: disk and bulge sources lensed by bulge, M31 halo and Galactic halo lenses. We confirm the high optical depth and the strong optical depth gradient along the M31 minor axis due to a dark halo of lenses and also discuss the magnitude of the self-lensing due to the bulge. We explore how the shape of the optical depth maps to M31 vary with the halo parameters core radius and flattening.

## 1 INTRODUCTION

The ongoing microlensing observations towards the LMC and SMC have provided extremely puzzling results. On the one hand, analysis of the first two years of observations (Alcock et al. 1997a) suggest a halo composed of objects with mass  $\sim 0.5M_{\odot}$  and a total mass in MACHOs out to 50 kpc of around  $2.0 \times 10^{11}M_{\odot}$ . On the other hand, producing such a halo requires extreme assumptions about star formation, galaxy formation, and the cosmic baryonic mass fraction. An attractive possibility is that the microlenses do not reside in the halo at all! Alternative suggested locations are the LMC halo (Kerins & Evans 1999), the disk of the LMC itself (Sahu 1994), a warped and flaring Galactic disk (Evans et al. 1998), or an intervening population (Zhao 1998). Unfortunately, the low event rates, uncertainties in the Galactic model, and the velocity-mass-distance degeneracy in microlensing all conspire to make precise determinations of the MACHO parameters difficult. Over the next decade, second generation microlensing surveys, monitoring ten times the number of stars in the LMC will improve the overall statistics (and numbers of “special” events) considerably, allowing an unambiguous determination of the location of the microlenses. Even so, the paucity of usable lines of sight within our halo makes determination of the halo parameters such as the flattening or core radius very difficult.

The Andromeda Galaxy (M31) provides a unique laboratory for probing the structure of galactic baryonic halos (Crotts 1992). Not only will the event rate be much higher than for LMC lensing, but it will be possible to probe a large variety of lines of sight across the disk and bulge and though the M31 halo. Furthermore, it provides another example of a bulge and halo which can be studied, entirely separate from the Galaxy. Recently, two collaborations, MEGA and AGAPE, have begun observations looking for microlensing in the stars of M31. Previous papers have made it clear that a substantial microlensing signal can be expected. In this pa-

per we calculate, using realistic mass models, optical depth maps for M31. The results suggest that we should be able to definitively say whether M31 has a dark baryonic halo with only a few years or less of microlensing data. We also discuss how their variation with halo parameters may allow us to determine the M31 halo structure. This is particularly important in evaluating the level of resources that should be dedicated towards the ongoing observational efforts. Preliminary results suggest that the core radius and density profile power-law should be the easiest parameters to extract.

The paper is organized in the following manner. In the next section we briefly discuss the M31 models we used. Following this we present optical depth maps for various halo models, discuss the microlensing backgrounds and finish with a quick discussion of the implications of the maps.

## 2 MODELING

Sources are taken to reside in a luminous two-component model of M31 consisting of an exponential disk and a bulge. The disk model is inclined at an angle of  $77^{\circ}$  and has a scale length of 5.8 kpc and a central surface brightness of  $\mu_R = 20$  (Walterbos & Kennicutt 1988). The bulge model is based on the “small bulge” of Kent (1989) with a central surface brightness of  $\mu_R = 14$ . This is an axisymmetric bulge with a roughly  $\exp(-r^{0.4})$  falloff in volume density with an effective radius of approximately 1 kpc and axis ratio,  $c/a \sim 0.8$ . Values of the bulge density are normalized to make  $M_{bulge} = 4 \times 10^{10}M_{\odot}$ .

The predominant lens population is taken to be the M31 dark matter halo. We explore a parametrized set of M31 halo models. Each model halo is a cored “isothermal sphere” determined by three parameters: the flattening ( $q$ ), the core radius ( $r_c$ ) and the MACHO fraction ( $f_b$ ):

arXiv:astro-ph/9904314v2 24 Apr 1999

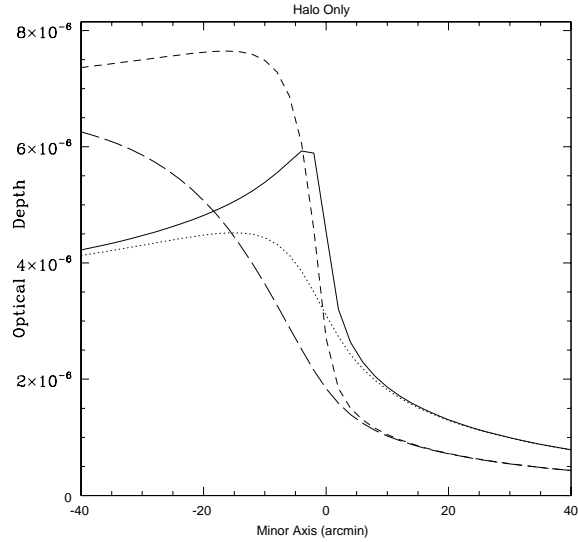


**Figure 1.** Halo optical depth along the minor axis. The curves are: solid line –  $q=0.3$  core=1kpc, dotted line –  $q=0.3$  core= 5kpc, dashed line –  $q=1.0$  core=1.0kpc, and long dashed line –  $q=1.0$  core=5.0kpc

$$\rho(x, y, z) = \frac{V_c(\infty)^2}{4\pi G} \frac{e}{a^2 q \sin^{-1} e} \frac{1}{x^2 + y^2 + (z/q)^2 + a^2}, \quad (1)$$

where  $a$  is the core radius,  $q$  is the  $x$ - $z$  axis ratio,  $e = \sqrt{1 - q^2}$  and  $V_c(\infty) = 240\text{km/s}$  is taken from observations of the M31 disk. In section 4 we briefly consider the optical depth due to other populations such as the bulge stars.

More details of our modeling are given in Gyuk & Crotts (1999) where in particular the velocity distributions (necessary for calculation of the microlensing rate) are discussed. These considerations do not affect the optical depths treated here.

### 3 OPTICAL DEPTH MAPS

The classical microlensing optical depth is defined as the number of lenses within one Einstein radius of the source-observer line-of-sight (the microlensing tube):

$$\tau = \int_0^D \frac{\rho_{\text{halo}}(d)}{M_{\text{lens}}} \frac{4GM_{\text{lens}}}{c^2} \frac{(D-d)}{D} dd \quad (2)$$

Such a configuration is intended to correspond to a “detectable magnification” of at least a factor of 1.34. Unfortunately, in the case of non-resolved stars (“pixel lensing”) we have typically

$$\pi\sigma^2 S_{M31} \gg L_*. \quad (3)$$

where  $S_{M31}$  is the background surface brightness,  $4\pi\sigma^2$  is the effective area of the seeing disk and  $L_*$  is the luminosity of the source star. Thus it is by no means certain that a modest increase of  $L_* \rightarrow 1.34L_*$ , as the lens passes within an Einstein radius, will be detectable. Furthermore, even for the events detected, measurement of the Einstein timescale  $t_0$  is difficult. Thus measurement of the optical depth may be difficult. Nonetheless, advances have been made in constructing estimators of optical depth within highly crowded star fields

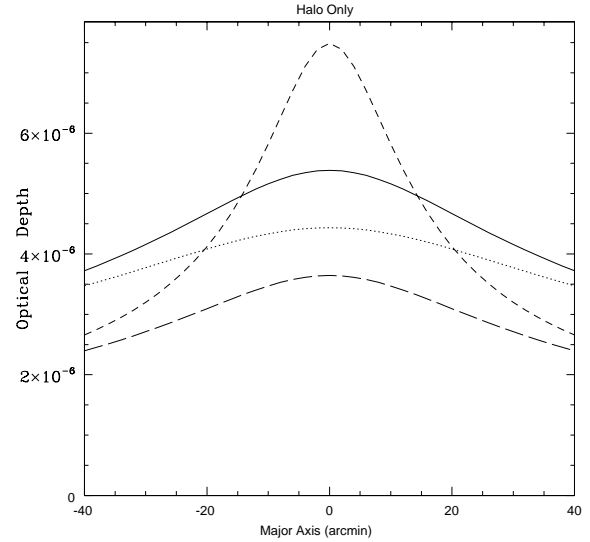


**Figure 2.** Optical depth along a line parallel to the major axis and offset along the minor axis by  $-10'$  (towards the far side of the disk). The curves are: solid line –  $q=0.3$  core=1kpc, dotted line –  $q=0.3$  core= 5kpc, dashed line –  $q=1.0$  core=1.0kpc, and long dashed line –  $q=1.0$  core=5.0kpc

(Gondolo 1999), which do not require the Einstein timescale for individual events, although they still require evaluation of the efficiency of the survey in question for events with various half maximum timescales. The errors on the derived optical depths will likely be larger than for the equivalent number of classical microlensing events. It is clear, however, that image subtraction techniques (Tomaney & Crotts 1996, Alcock et al. 1999a, b) can produce a higher event rate than conventional photometric monitoring. Thus one needs models of the optical depth, even if expressed only in terms of the cross-section for a factor 1.34 amplification in order to understand how microlensing across M31 will differ depending on the spatial distribution of microlensing masses in the halo and other populations.

The above expression for the optical depth must be slightly amended to include the effects of the three-dimensional distribution of the source stars, especially of the bulge. We thus integrate the source density along the line of sight giving

$$\tau = \frac{\int_0^\infty \rho(S) \int_0^S \frac{\rho_{\text{halo}}(s)}{M_{\text{lens}}} \frac{4GM_{\text{lens}}}{c^2} \frac{(S-s)}{S} ds dS}{\int_0^\infty \rho(S) dS} \quad (4)$$

The results of this calculation as a function of position for a variety of halo models are shown in Figure 3. The most important attribute is the strong modulation of the optical depth from the near to far side of the M31 disk as was first remarked on by Crotts (1992). Near-side lines-of-sight have considerably less halo to penetrate and hence a lower optical depth. This can be seen nicely in Figure 1 where we plot the optical depth along the minor axis for the four models depicted in Figure 3. While all models exhibit the strong variation from near to far, the fractional variation in  $\tau$  across the minor axis is most pronounced for less flattened models, and changes in  $\tau$  along the minor axis occur most rapidly for models with small core radii. This can be understood

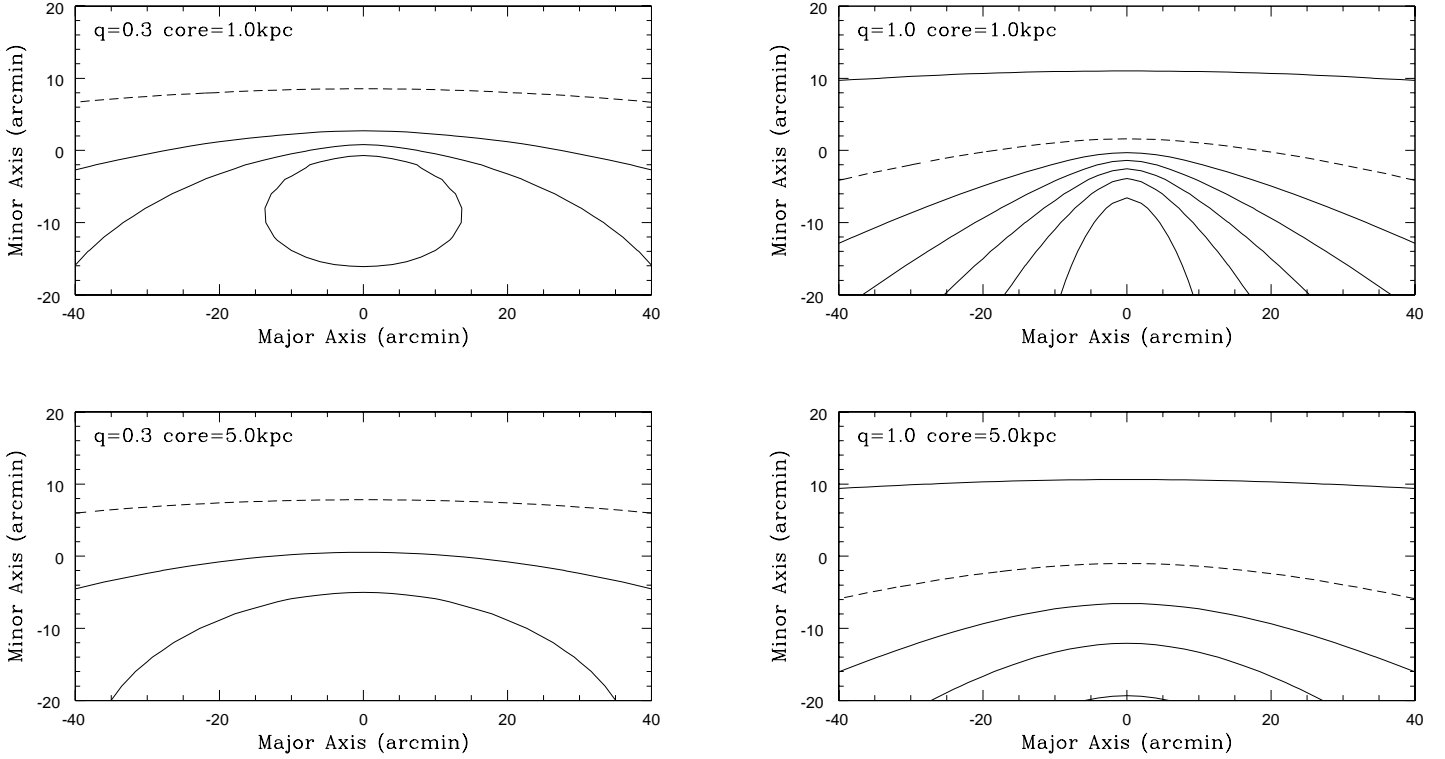


**Figure 3.** Contours of optical depth for halo models a)  $q=0.3$  core=1.0, b)  $q=0.3$  core=5.0, c)  $q=1.0$  core=1.0 halo and d)  $q=1.0$  core=5.0. Contours are from top to bottom: a)  $2,3,4$  and  $5 \times 10^{-6}$ , b)  $2,3$  and  $4 \times 10^{-6}$ , c)  $1,2,3,4,5,6$  and  $7 \times 10^{-6}$  and d)  $1,2,3,4$  and  $5 \times 10^{-6}$ . For all models the dashed contour is  $2.0 \times 10^{-6}$ .

geometrically: in the limit of an extremely flattened halo the pathlength (and density run) through the halo is identical for locations equidistant from the center. Small core radii tend to make the central gradient steeper and produce a maximum at a distance along the minor axis comparable to the core size. This maximum is especially prominent in the flattened halos.

Variations in core radii and flattening are also reflected in the run of optical depth along the major axis. In Figure 2 we show the optical depth along the major axis displaced by  $-10'$  on the minor axis. The gradients in the small core radii models are much larger than for large core radii. Asymptotically the flattened halos have a larger optical depth.

#### 4 BACKGROUND LENSING

Unfortunately, the M31 halo is not the only source of lenses. As mentioned above, the bulge stars can also serve as lenses. We show in Figure 4 the optical depth contributed by the bulge lenses. The effect of the bulge lenses is highly concentrated towards the center. This is a mixed blessing. On the one hand the bulge contribution can thus be effectively removed by deleting the central few arcminutes of M31. Beyond a radius of 5 arcminutes, bulge lenses contribute negligibly to the overall optical depth. On the other hand the source densities are much higher in the central regions and thus we expect the bulk of our halo events to occur in these regions. We discuss this point in more detail in a forthcoming

paper (Gyuk & Crots 1999). The bulge of M31 might easily serve as an interesting foil to the Galactic Bulge, which produces microlensing results which seem to require a special geometry relative to the observer, or other unexpected effects (Alcock et al. 1997b, Gould 1997).

In addition to the M31 bulge lensing a uniform optical depth across the field will be contributed by the Galactic halo. This contribution will be of order  $\sim 10^{-6}$  corresponding to a 40% Galactic halo as suggested by the recent LMC microlensing results. Finally, disk self lensing will occur. The magnitude of the optical depth for this component will however be at least an order of magnitude lower than the expected halo or bulge contributions (Gould 1994) and hence is ignored in these calculations.

#### 5 DISCUSSION AND CONCLUSIONS

The optical depth maps for M31 shown above exhibit a wealth of structure and clearly contain important information on the shape of the M31 halo. The most important of these information bearing characteristics is the asymmetry in the optical depth to the near and far sides of the M31 disk. A detection of strong variation in the optical depth from front to back will be a clear and unambiguous signal of M31's microlensing halo, perhaps due to baryons. No other lens population or contaminating background can produce this signal. However, the lack of a strong gradient should not be taken as conclusive proof that M31 does not have a

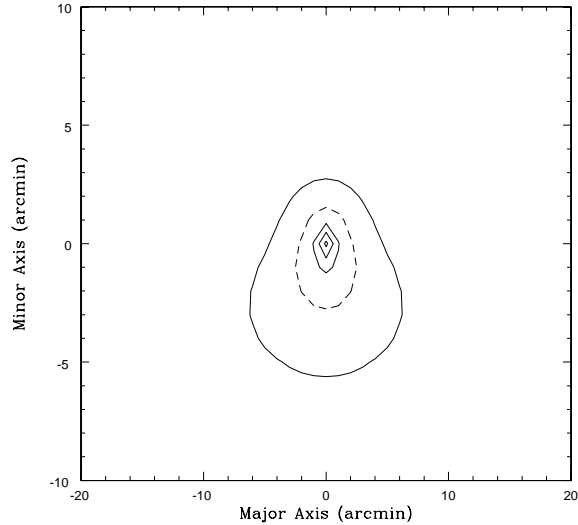


**Figure 4.** Contours of optical depth for the bulge self-lensing. Contours are, from the outside in:  $1, 2, 3, 4$  and  $5 \times 10^{-6}$ . Note that the region shown is half the dimensions of the maps of Figure 3.

halo. As discussed above, strong flattening or a large core radius can reduce or mask the gradient. Nevertheless, the halo should still be clearly indicated by the high microlensing rates observed outside the bulge region. In such a case, however, careful modeling of the experimental efficiency and control over the variable star contamination will be necessary to insure that the observed event are really microlensing.

Further information about the structure of the M31 baryonic halo can be gleaned from the distribution of microlensing along the major axis. A strong maximum at the minor axis is expected for small core radii especially for spherical halos.

The combination of the change in event rate both along the major and minor axis directions can in principle reveal both the core radius and flattening from a microlensing survey. How easily such parameters can be measured depends critically on the rate at which events can be detected, which we discuss in paper II of this series, along with estimates of the expected accuracy. Additionally, we will discuss strategies to optimize such surveys for measuring shape parameters.

## REFERENCES

- Alcock, C. et al. 1997a, *ApJ*, 486, 697  
 Alcock, C. et al. 1997b, *ApJ*, 479, 119  
 Alcock et al. 1999a, astro-ph/9903215  
 Alcock et al. 1999b, astro-ph/9903219  
 Crotts A.P.S., 1992, *ApJ*, 395, L25  
 Evans et al. 1998, *ApJ* in press, astro-ph/9711224  
 Gondolo, P. 1999. *ApJ*, 510, L29  
 Gould, A., 1994, *ApJ*, 435, 573  
 Gould, A., 1997, in *Astronomical Time Series*, eds.D. Maoz, A. Sternberg, and E.M. Leibowitz, p.37  
 Kent, S. 1989, *AJ*, 97, 1614  
 Kerins, E. J., & Evans, N. W., 1999, *ApJ* in press, astro-ph/9812403

- Sahu, K.C., 1994, *PASP*, 106, 942  
 Tomaney, A. & Crotts, A.P.S. 1996, *AJ*, 112, 2872  
 Waltherbos, R.A.M. & Kennicutt 1988, *A&A*, 198, 61  
 Zhao, H., 1998, *MNRAS*, 294, 139